

Alterations in Water Structure Induced by Guanidinium and Sodium Ions<sup>†</sup>

Raymond D. Mountain\*

*Physical and Chemical Properties Division, National Institutes of Standards and Technology, Gaithersburg, Maryland 20899-8380*

D. Thirumalai

*Institute of Physical Science and Technology, University of Maryland, College Park, Maryland 20742**Received: July 29, 2004; In Final Form: September 10, 2004*

Using molecular dynamics simulations, we have probed the ion-induced changes in the water structure as the concentration of ion is varied. We consider two ions, namely, sodium chloride and guanidinium chloride. As the concentration of sodium ions,  $\text{Na}^+$ , is increased the water structure is greatly perturbed. When the mole fraction of water is less than about 0.93, the tetrahedral network of water is affected and there is a total disruption of the tetrahedral structure of water, just as found in water at high pressures. The number of water–water hydrogen bonds per water molecule is greatly diminished as  $\text{Na}^+$  concentration increases. Surprisingly, we find that the number of water molecules that are coordinated to  $\text{Na}^+$  is nearly independent of the sodium chloride concentration. In contrast to the kosmotropic ion  $\text{Na}^+$ , the weakly hydrated chaotropic ion  $\text{Gdm}^+$  does not alter the water structure as dramatically. At all  $\text{Gdm}^+$  concentrations examined here, the water hydrogen bonds are fully preserved. We find that the tetrahedral network of water is compromised only at the highest  $\text{Gdm}^+$  concentration. The differences in the interaction of these two ions with water as their concentration is varied are used to propose a mechanism by which  $\text{Gdm}^+$  denatures proteins.

## 1. Introduction

The interactions of ions with water is important in a variety of biological systems. The structure and stability of the hydrated ions determine their interaction with proteins and nucleic acids.<sup>1,2</sup> The efficiency of denaturation of proteins by ions is dependent on the strength of their interactions with water. Over a century ago, Hofmeister arranged ions according to their ability to salt-in (enhance protein stability) or salt-out proteins (for a review see ref 3). For example, it is predicted that the weakly hydrated, planar guanidinium ion,  $\text{Gdm}^+$  ( $\text{C}(\text{NH}_2)_3^+$ ), should be efficient in denaturing proteins whereas ions such as  $\text{SO}_4^{2-}$  would not be a denaturant. Because hydrophobic interactions are believed to be the dominant determinants of the stability of proteins, the Hofmeister effect is sometimes explained by the effect ions have in modulating the effective hydrophobic interactions. The situation is more complicated because of the opposing effects ions typically have on peptide groups and hydrophobic moieties.<sup>3,4</sup>

The effect of ions to salt-in or salt-out proteins depends to a large extent on its hydration properties. Collins<sup>5,6</sup> proposed that strongly hydrating ions (kosmotropes) would not interact with hydrophobic moieties whereas weakly hydrated ions (chaotropes) would interact with hydrophobic species. Because hydration properties are determined by charge densities, it follows that the ability of ions to stabilize or destabilize proteins is determined by valence, size, and shape. The shape of the ion is important because the interaction of an ion with proteins is determined by the interplay of ion–water, water–water, and ion–protein interactions. Because all these interactions are ultimately related to the ability of the solvent and ions to form

suitable hydrogen bonds, the shape of ion plays an important role as well. In addition to protein stability, the selectivity of ion channels for certain ions also depends on the hydration state. For example, removal of water from the strongly hydrated ion  $\text{Na}^+$  is free-energetically prohibitive while partial dehydration of the larger  $\text{K}^+$  ion is facile. The contrasting behavior of the monovalent cations serves as a possible selection mechanism for particular ions in ion channels. These observations show that understanding hydration of ions in terms of their chemical structure is important in describing their interactions with biologically important molecules.

In general, when molecules are dissolved in water, the immediate environment of the molecule depends strongly on the way the molecule interacts with water molecules. Ions, and to a lesser extent, polar molecules, interact sufficiently strongly that the hydrogen bond network of water is *locally* modified. At the other extreme, hydrophobic species such as rare gas atoms and alkane molecules tend to be excluded from contact with water molecules to the maximum extent possible and are said to have hydrophobic interactions. This briefly explains why ions and polar molecules are readily soluble in water and why rare gases and alkanes are not.

The hydration of ions is, to a first approximation, determined by its charge density.<sup>5</sup> The larger charge density of  $\text{Na}^+$  makes it a more strongly hydrated ion compared to  $\text{K}^+$ . As a result, ions which are kosmotropic would tend to order the water molecules locally. It follows that, as the concentration of ions is increased, kosmotropic ions can substantially alter the water structure. On the other hand, the opposite trend is expected for chaotropic ions. In particular,  $\text{Gdm}^+$ , at moderate concentrations, should not greatly alter the water structure which is in accord with recent neutron scattering experiments.<sup>7</sup> For several problems of interest, it is necessary to understand the changes in

<sup>†</sup> Part of the special issue "Frank H. Stillinger Festschrift".

\* Corresponding author. E-mail: RMountain@nist.gov.

**TABLE 1: The Lennard-Jones Parameters Used in the Simulation<sup>a</sup>**

sites	$\epsilon/k_B$ , K	$\sigma$ , nm
O–O	78.24	0.3166
Na–Na	68.38	0.2720
Cl–Cl	183.8	0.3549
O–Na	73.15	0.2943
O–Cl	119.9	0.3357
Na–Cl	112.1	0.3134

<sup>a</sup> O and H stand for the oxygen and hydrogen sites on the water molecule and Na and Cl stand for the ions  $\text{Na}^+$  and  $\text{Cl}^-$ . For this model, there is no Lennard-Jones interaction involving the H-sites. In units of the charge on the proton, the charge on the O-site is  $-0.8476$  and on the H-site is  $0.4238$ . The charge on the ions is Na,  $+1$  and Cl,  $-1$ .

hydration of ions with varying charge density as the ion concentration increases. Although  $\text{Gdm}^+$  is an efficient denaturant, concentrations exceeding one or two molar  $\text{Gdm}^+$  are typically required to destabilize proteins. At the elevated ion concentrations, less is known about how the presence of the solute molecules modifies the structure of the water molecules as the concentration of the solute increases. In this paper, we discuss the results of molecular dynamics simulations that address the question of how water structure, as reflected in the pair correlation functions, is modified as the amount of solute varies. The solutes considered are sodium chloride and guanidinium chloride. The weakly hydrated  $\text{Gdm}^+$  denatures proteins while high concentrations of sodium can salt-out proteins. These two ions offer opposing case studies for probing the nature of the hydration of ions. Before undertaking an investigation of the way guanidinium chloride denatures proteins, we feel that it is important to examine how these solutes modify the structure of water and in particular identify any differences between sodium chloride and guanidinium chloride driven changes.

## 2. Methods

**Models.** We used the standard SPC/E model for water.<sup>8</sup> In this rigid three-site model, the hydrogen atoms are  $0.1$  nm from water and the HOH angle is  $109.47^\circ$ . The partial charges on oxygen and hydrogen are  $q_O = -0.8476e$  and  $q_H = 0.4238e$ , respectively. The Lennard-Jones (LJ) parameters for the oxygen sites are  $\epsilon_O = 0.037$  kJ/mol and  $\sigma_O = 0.3166$  nm. The interaction between intermolecular sites  $i$  and  $j$  on the ions that are separated by a distance  $r$  is

$$\phi_{ij}(r) = q_i q_j / r + 4\epsilon_{ij}[(\sigma_{ij}/r)^{12} - (\sigma_{ij}/r)^6]$$

The ion potentials consist of a Lennard-Jones potential plus a point charge at the ion site. We consider here the ions  $\text{Na}^+$  and  $\text{Cl}^-$ .<sup>9</sup> Ion–water interactions were obtained using the Lorentz–Berthelot combining rules.<sup>10</sup> The parameters for the potentials are listed in Table 1. The potential parameters have not been tuned to a particular property of the ion–water mixtures with the consequence that trends rather than explicit details are the focus of this work.

We used the OPLS-AA model for the guanidinium ions ( $\text{C}(\text{NH})_2^+$ ) with an additional weak Lennard-Jones interaction between the ion hydrogen sites and all other sites to stabilize the system during the equilibration phase of the simulations.<sup>11</sup> The parameters for the  $\text{Cl}^-$  ion are taken from Straatsma.<sup>12</sup> The potential parameters for guanidinium chloride are listed in Table 2. Both the water molecules and the guanidinium ions were treated as rigid, planar objects. As before, the  $\text{Gdm}^+$ –water interactions were obtained using the combining rules.

**TABLE 2: The Potential Parameters for the OPLS-AA Guanidinium Ion Model and for the  $\text{Cl}^-$  Ion Are Listed for the Atom Types<sup>a</sup>**

atom	$\epsilon$ , K	$\sigma$ , nm	$q$ , ( $ e $ )
C	25.2	0.225	0.64
N	85.6	0.325	$-0.80$
H <sup>b</sup>	15.6	0.205	0.46
$\text{Cl}^-$	64.8	0.375	$-1.0$

<sup>a</sup> The unlike pair parameters are obtained using the geometric mean mixing rule for both the  $\epsilon$  and  $\sigma$  parameters. <sup>b</sup> It was necessary to have a small Lennard-Jones term for the hydrogen sites on the ion to keep the water–oxygen ion–hydrogen separations from becoming too small.

**Simulation Details.** A series of simulations were made for six sodium chloride concentrations. There were a total of 216 ions plus water molecules in each case. The compositions were 1 Na ion, 1 Cl ion, and 214 water molecules; 2 Na ions, 2 Cl ions, and 212 water molecules; 4 Na ions, 4 Cl ions, and 208 water molecules; 8 Na ions, 8 Cl ions, and 200 water molecules; 11 Na ions, 11 Cl ions, and 194 water molecules; and 16 Na ions, 16 Cl ions, and 184 water molecules. The mole fractions of water,  $X_W$ , are 0.991, 0.982, 0.963, 0.926, 0.898, and 0.852, respectively, with the  $\text{Na}^+$  and  $\text{Cl}^-$  ions treated as separate components of the mixture. The last composition is close to the experimentally determined saturation condition.<sup>13</sup>

Four separate simulations have been made for aqueous guanidinium chloride solution. In each case, the total number of molecules plus ions is 1000. The compositions of the cases are 998 water and 1 each of the guanidinium and chloride ions, 900 water and 50 each of the ions, 850 water and 75 each of the ions, and 800 water and 100 each of the ions. Since the guanidinium chloride is in the form of distinct, separated ions, we determine the mole fractions of each component separately. The mole fractions for water,  $X_W$ , are 0.998, 0.900, 0.850, and 0.800 with the corresponding mole fractions for each of the ions being 0.001, 0.05, 0.075, and 0.10. The results reported here for a single guanidinium ion with water are consistent with the results of Boudon et al. who used a different set of potential parameters.<sup>14</sup> The details of the MD simulations are the same as in the NaCl studies.

These compositions maintain overall charge neutrality of the system, a necessary condition for the Ewald method used to describe the Coulomb interactions to converge.<sup>15</sup> The equations of motion were integrated using an iterated form of the Beeman algorithm<sup>16,17</sup> with a time step of 1 fs.<sup>18</sup> Quaternions were used to describe the orientational motion of the water molecules.<sup>19–21</sup> The temperature of the system was maintained by Nosé–Hoover thermostats for the translational and orientational degrees of freedom.<sup>22</sup> In each case, the volume of the simulation cell was adjusted so that the calculated pressure was within  $\pm 2$  MPa of zero. Considerable care was taken to “equilibrate” the system before taking samples. Because this work has focused on the structure of water, a 100 ps production run suffices.

## 3. Results

To probe the structural changes in water as a function of concentration of  $\text{Na}^+$  and  $\text{Gdm}^+$ , we have calculated the three site–site pair functions for water,  $g_{HH}(r)$ ,  $g_{OH}(r)$ , and  $g_{OO}(r)$ . All pair functions are normalized to approach unity at large distances by dividing the square of the water mole fraction  $X_W$ . Subscripts in the pair functions refer to atom sites on water.

**How  $\text{Na}^+$  and  $\text{Cl}^-$  Affect Water Structure.** The solvation of  $\text{Na}^+$  and  $\text{Cl}^-$  in infinite dilution has been extensively studied using computer simulations. However, much less is known about

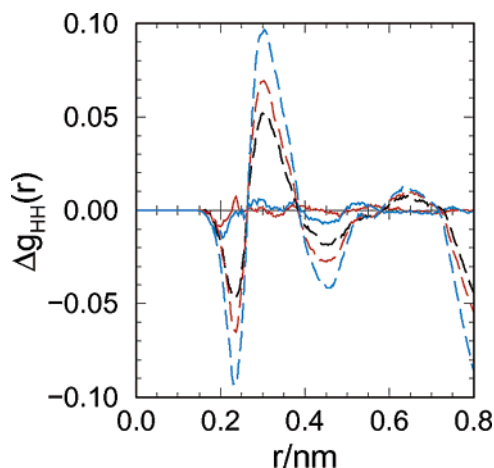


**Figure 1.** The differences  $\Delta g_{HH}(r)$  are shown as functions of  $r$ . The solid curve is for  $X_W = 0.981$ , the dotted curve is for  $X_W = 0.963$ , the dashed curve is for  $X_W = 0.926$ , the long dashed curve is for  $X_W = 0.898$ , and the long-short dashed curve is for  $X_W = 0.852$ .

how the structure of water is modified by the presence of these ions as their concentration is increased.

$g_{HH}(r)$ . First consider the pair functions between hydrogen atoms. Neutron scattering experiments by Leberman and Soper (LS)<sup>23</sup> show that there are considerable changes in  $g_{HH}(r)$  as the concentration of  $\text{Na}^+$  is increased. Following LS, we plot in Figure 1  $\Delta g_{HH}(r) = g_{HH}(r; [\text{Na}^+]) - g_{HH}(r; [0.0046])$ , where  $[\text{Na}^+]$  refers to the mole fraction of  $\text{Na}^+$  ions. This figure shows that as the  $\text{Na}^+$  concentration increases there is a decrease in the peak height at  $r \approx 0.23$  nm and an enhancement of the first minimum at  $r \approx 0.32$  nm. The diminishing of the peak at  $r \approx 0.23$  nm is indicative of the decrease in the orientational ordering of a pair of hydrogen-bonded water molecules. Such a decrease is also reflected in the increase in the minimum at  $r \approx 0.32$  nm. The mole fraction of water squared factor has been removed from each of the  $g_{HH}(r)$  functions before the difference was taken.

Water becomes disordered at high pressure and temperature. Pressure-induced disordering also results in changes in  $g_{HH}(r)$  similar to that found for ionic solutions. The analogy between pressure effects and ionic solutions was proposed by Leberman and Soper who mapped the ion concentration to equivalent values of pressure. In this picture, the increase in  $[\text{Na}^+]$  can be thought of as an increase in pressure. This, in turn, decreases the orientational order.

$g_{OO}(r)$ . As the concentration of  $\text{Na}^+$  increases, there is a profound change in the water pair functions as indicated in Figure 2 for  $g_{OO}(r)$ . The height of the first peak in  $g_{OO}(r)$  decreases dramatically with increasing  $\text{Na}^+$  concentration which indicates the disruption of the water structure. The pronounced second maximum at  $r = 0.44$  nm is the signature of a high degree of correlation between second neighbor molecules at positions corresponding to vertexes of a tetrahedron with a first neighbor molecule at the geometrical center of the tetrahedron. This indicates that locally, water molecules are predominantly tetrahedrally ordered. At large values of  $X_W$  ( $> 0.93$ ), the peak at  $r = 0.44$  nm, which is a signature of the tetrahedral network, is preserved. When  $X_W = 0.93$ , the second maximum is greatly reduced implying that the short range order associated with tetrahedral coordination has been disrupted. Further increase in the NaCl concentration greatly reduces this structural feature. Near the saturation concentration of NaCl, this feature is absent.

Zhu and Robinson<sup>24</sup> also found, using a different water and salt model, that for a 1.79 molality NaCl solution, the tetrahedral

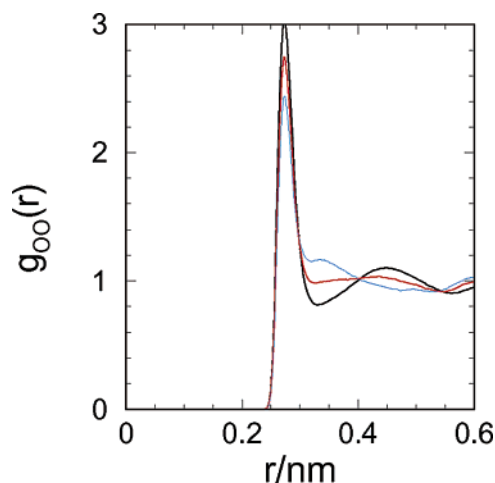


**Figure 2.** The oxygen–oxygen pair functions are shown for three of the compositions with the  $X_W = 0.991$  (black curve), 0.926 (red curve), and 0.852 (blue curve). The curves for the other compositions lie between these three curves with the heights of the principal maximum decreasing with decreasing water fraction.

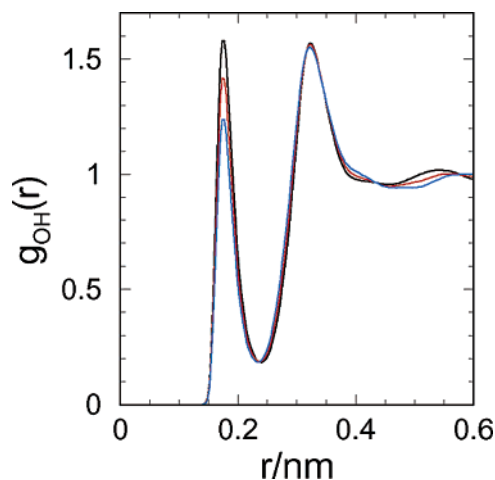


**Figure 3.** The hydrogen–oxygen pair functions are shown for three of the compositions with the  $X_W = 0.991$  (black curve), 0.926 (red curve), and 0.852 (blue curve). The curves for the other compositions lie between these three curves with the heights of the first maximum decreasing with decreasing water fraction.

network of water structure is disrupted. However, they did not probe the changes in the structure of water as the concentration of  $\text{Na}^+$  is altered. Recently, Sherman and Collings<sup>25</sup> examined NaCl brines over a wide range of temperature, pressure, and composition ranges. For 298 K, 0.1 MPa, and near saturation concentration of NaCl, the structure of the  $g_{OO}$  pair function has changed much like that indicated in Figure 2. Weerasinghe and Smith have used Kirkwood–Buff integrals to determine a set of potential parameters for  $\text{Na}^+$  and  $\text{Cl}^-$ .<sup>26</sup> They too find that the structure of  $g_{OO}$  is modified at high ion concentrations as indicated in Figure 2.

$g_{OH}(r)$ . Changes in the hydrogen bond formation between water molecules are best monitored by computing  $g_{OH}(r)$ . In Figure 3, we show  $g_{OH}(r)$  as a function of  $r$  in varying salt concentrations. At all values of  $\text{Na}^+$  concentration, there is a peak at  $r \approx 0.18$  nm which is the characteristic signal of hydrogen bond formation between water molecules. However, the amplitude of the peak is greatly diminished as  $\text{Na}^+$  concentration increases. The number of hydrogen bonds between water molecules (obtained by integrating  $g_{OH}(r)$  from  $r = 0$  to  $r \approx 0.26$  nm) changes from 3.4 to 2.7 as  $X_W$  decreases from

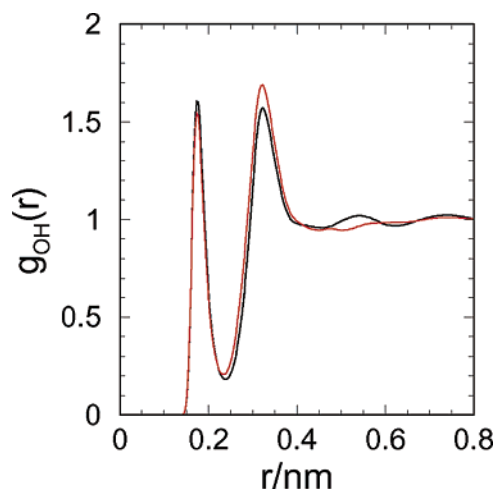


**Figure 4.** The hydrogen–oxygen pair functions are shown for two guanidinium chloride compositions with the largest mole fraction of water (black line) and the smallest (red line). The intermediate composition cases lie between these curves.

0.991 to 0.852. The drastic decrease in the number of hydrogen bonds is another evidence of ion-induced disruption of water structure. The drastic alteration of water structure at high  $\text{Na}^+$  concentrations may be a contributing factor in the ability of sodium chloride to precipitate proteins.

**Coordination Number of  $\text{Na}^+$ .** Because of the relatively high charge density, sodium ions are strongly hydrated. At low  $\text{Na}^+$  concentration, we expect that sodium is coordinated with six water molecules. By integrating the  $g_{\text{Na}^+\text{O}}(r)$  pair function, we find that the coordination number  $\text{Na}^+$  is nearly independent of the ion concentration. The mean value of the coordination number is between 5.7 and 6. This is consistent with the results of Dreisner, et al.<sup>27</sup> for a slightly different water and NaCl model at ambient conditions. Thus, the disordering of water structure does not change the hydration of  $\text{Na}^+$  even at high ionic concentration. However, at much higher temperature and high salt concentration, ion pairing between  $\text{Na}^+$  and  $\text{Cl}^-$  is facilitated because of a decrease in the water dielectric constant.<sup>27,25</sup>

**Water Structure in the Presence of Guanidinium Chloride. Pair Functions for Water.** To probe the changes in the water structure because of the presence of guanidinium ions, we have computed the appropriate radial distribution functions for water. On the basis of charge density considerations, we expect  $\text{Gdm}^+$  to be weakly hydrated. This implies that the hydrogen bonds between water molecules are stronger than between the amide protons on  $\text{Gdm}^+$  and water oxygen atoms. As a result, the structure of water is not expected to be greatly perturbed, at least at low  $\text{Gdm}^+$  ion concentrations. These expectations are borne out in  $g_{\text{OH}}(r)$  pair function (Figure 4) which shows that the peak positions do not change as the concentration of  $\text{Gdm}^+$  increases. More importantly, the peak height in the first maximum, at the typical hydrogen bond distance, is virtually unchanged. As the concentration of  $\text{Gdm}^+$  increases, there are small, but insignificant, changes in the second peak. From these results, we conclude that even at elevated concentrations  $\text{Gdm}^+$  does not alter the hydrogen bond patterns between water molecules to the extent that concentrated solutions of NaCl do.

In Figure 5, we plot  $\Delta g_{\text{HH}}(r) = g_{\text{HH}}(r; [\text{Gdm}^+]) - g_{\text{HH}}(r; [0.001])$  as a function of  $r$ . However, unlike  $\text{Na}^+$ , the amplitude of the first peak is not diminished as the  $\text{Gdm}^+$  concentration is enhanced. Surprisingly, in the presence of  $\text{Gdm}^+$  the amplitude of the first peak in  $g_{\text{HH}}(r)$  at  $r \approx 0.23$  nm

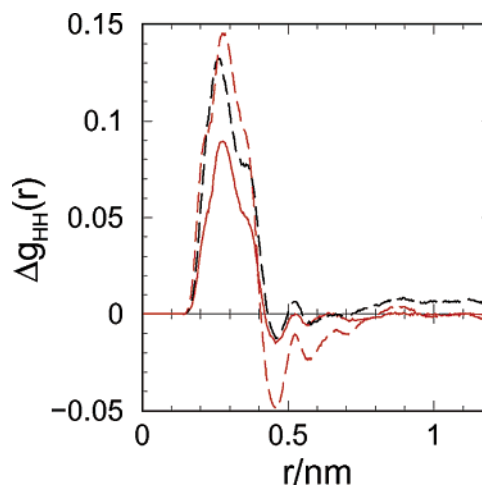


**Figure 5.** The difference in the water hydrogen–hydrogen pair functions for various compositions of guanidinium chloride. The dashed line is for 900 water molecules and 50 each of the ions. The long dashed line is for 850 water molecules and 75 each of the ions. The long–short dashed line is for 800 water molecules and 100 each of the ions.

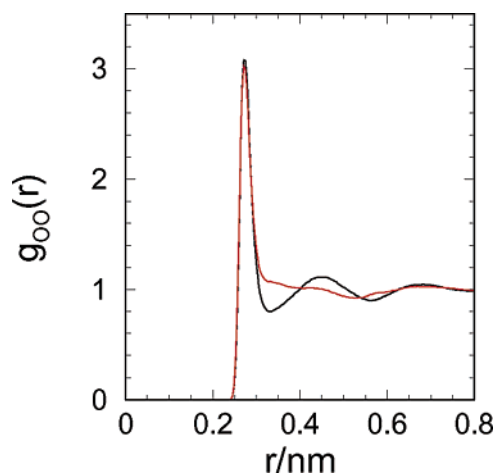


**Figure 6.** The oxygen–oxygen pair functions for two compositions in the presence of guanidinium chloride. The black line is for 998 water molecules and 1 each of the ions and the red line is for 800 water molecules and 100 each of the ions. The curves for the intermediate compositions lie between these curves.

increases. This implies that as the  $\text{Gdm}^+$  concentration increases the fluctuations in the network of water molecules engaged in hydrogen bonding are reduced. The enhancement of the first minimum at  $r \approx 0.45$  nm implies that at elevated  $\text{Gdm}^+$  concentrations, the orientational order of water is somewhat compromised. However, the effect is less for  $\text{Gdm}^+$  than for  $\text{Na}^+$ . To examine further the changes in the water structure, we have computed  $g_{\text{OO}}(r)$  as a function of  $\text{Gdm}^+$  concentration as shown in Figure 6. Interestingly, the amplitude of the first peak remains unaltered even at the highest  $\text{Gdm}^+$  concentration. The characteristics of the second peak in  $g_{\text{OO}}(r)$ , which signals the tetrahedral arrangement of water, are altered as  $\text{Gdm}^+$  increases. Although the mole fraction of the guanidinium ions has a larger range of values than was used for NaCl, the disruption of the water structure is less pronounced for equivalent mole fractions of water.

Weerasinghe and Smith, using a Kirkwood–Buff based model for the guanidinium chloride–water interaction, find that  $g_{\text{OO}}$  is not disrupted at high ion concentrations.<sup>28</sup>

**Hydrogen Bonds between Water and  $\text{Gdm}^+$ .** Since the disruption of the water structure is less pronounced for  $\text{Gdm}^+$



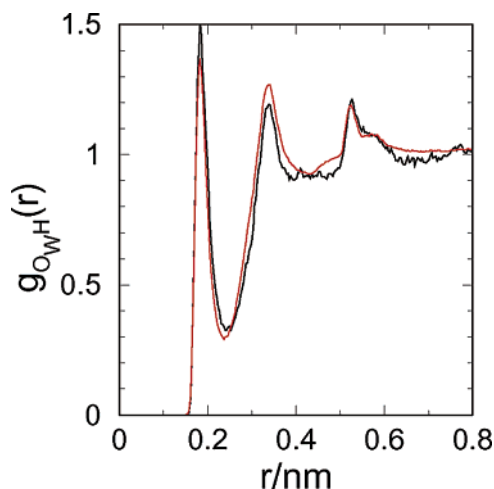


**Figure 7.** The oxygen water-guanidinium hydrogen pair functions for the highest and lowest water compositions are shown as normalized to unity for large separations. The solid curve is for  $X_W = 0.998$  and the dashed curve is for  $X_W = 0.80$ . The other two compositions are not shown as they lie between these two.

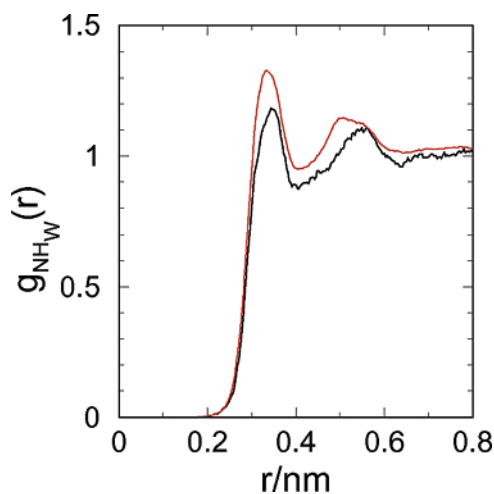


**Figure 8.** The guanidinium nitrogen water hydrogen pair functions for  $X_W = 0.998$  (black line) and for  $X_W = 0.80$  (red line). The curves are normalized to unity for large separation.

compared with the NaCl, it is of interest to examine other pair functions to see if this difference can be understood. To this end, we now examine how water is correlated with the hydrogen sites in the guanidinium ion. The oxygen water–guanidinium hydrogen pair functions,  $g_{OwH}(r)$  (H refers to the amide proton on  $Gdm^+$ ), show a clear hydrogen bond signature in the peak of these functions at  $r \approx 0.183$  nm (see Figure 7). These hydrogen bonds are longer than those between water molecules which supports the notion that  $Gdm^+$  is weakly hydrated. The structure of these curves is only weakly dependent on the composition once the overall composition dependence,  $X_W X_H$  is factored out so the functions approach unity for large distances.

Water can both donate and accept hydrogen bonds. The nitrogen sites do not accept hydrogen bonds from water because the first peak in  $g_{NHw}(r)$  occurs at a distance  $r \approx 0.35$  nm (Figure 8). This is reasonable as a water accepting a hydrogen bond has its hydrogen sites pointing away from the ion. A typical snapshot (Figure 9) shows that there are several water molecules interacting weakly with a  $Gdm^+$  ion. We find that the nitrogen sites do not form hydrogen bonds with other guanidinium ions as is evident from the corresponding pair functions (data not

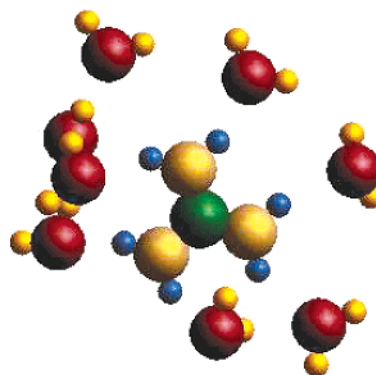


**Figure 9.** A snapshot of a guanidinium ion and the solvating water molecules that are within 0.4 nm of one of the hydrogens on the ion.

shown). This implies that  $Gdm^+$  ions do not self-associate but may interact by water-mediated contacts.

Since the hydrogen sites on both water and the guanidinium ion are positively charged, the negatively charged chloride ion can approach these sites with a maximum in the corresponding pair functions at 0.2 nm. To complete this picture, we note that the oxygen–nitrogen pair functions (not shown) indicate the closest approach of these sites is  $r \approx 0.25$  nm. Recent neutron scattering measurements on guanidinium chloride in water with a composition close to the 900 water molecule and 50 each for the ions case found no atoms closer to the nitrogen site than 0.28 nm.<sup>7</sup> Our simulation results are consistent with this observation.

#### 4. Conclusions

The kosmotrope,  $Na^+$ , a small ion with high charge density, and the chaotrope,  $Gdm^+$ , a relatively large ion with low charge density, affect water structure in a different manner. Although there are qualitative similarities in the changes in the pair functions of water induced by these ions, the quantitative differences have profound effect in their interactions with biological systems such as proteins and nucleic acids. The distortion of orientational order, as measured by the changes in  $g_{HH}(r)$ , is qualitatively different in the aqueous solutions of these ions. However, there are vast differences in the water hydrogen bond network induced by the two ions. As the concentration of  $Na^+$  increases, the strength of water–water hydrogen bond, as measured by changes in  $g_{OH}(r)$ , clearly decreases. In contrast, even at the highest  $Gdm^+$  ion concentrations, the amplitude of the first peak in  $g_{OH}(r)$  does not change which implies that the weakly hydrated  $Gdm^+$  ion does not alter the local network of water–water hydrogen bonds.

Predicting whether a given ion, at a specific ionic strength, stabilizes or destabilizes proteins is complicated by the opposing effects they have on peptide groups and hydrophobic residues. Kosmotropes tend to salt-out hydrophobic moieties<sup>29,30</sup> but tend to salt-in peptide groups.<sup>31</sup> The extent of these opposing effects, which are dependent on the ionic strength, determines the ability of ion to salt-in or salt-out proteins. For this reason, very high salt concentrations of NaCl are required to precipitate proteins as noted by Hofmeister over a century ago. These qualitative arguments are in accord with the Collins model<sup>5</sup> which predicts that ion interactions with proteins are determined by  $R_C = \epsilon_{IW}/\epsilon_{WW}$  where  $\epsilon_{IW}$  and  $\epsilon_{WW}$  are ion–water and water–water interaction strengths, respectively. Clearly,  $R_C > 1$  for  $Na^+$  and  $R_C < 1$  for  $Gdm^+$ .

There may not be a direct link between the extent to which a given ion induces alterations in water structure and its

denaturation efficiency.<sup>32</sup> The present work shows that, at a given concentration,  $\text{Na}^+$  induces larger changes in water structure than  $\text{Gdm}^+$ . Nevertheless,  $\text{Gdm}^+$  can efficiently denature proteins while  $\text{Na}^+$  can salt-out proteins only at sufficiently high concentration. A combination of factors including the extent of hydration and relative effects on hydrophobic and peptide group determines the efficiency of protein denaturation by ions. These parameters are a function of the shape of the ion. In addition, the total charge on the ion and how the charge is distributed on the sites of the molecule are also contributing factors.<sup>33</sup>

How does  $\text{Gdm}^+$  denature proteins? It is logical to suggest that  $\text{Gdm}^+$  must effect interactions with both the hydrophobic residues and the peptide group. Because  $\text{Gdm}^+$  ions do not self-associate and because they can engage in hydrogen bonds, we suggest that the possibility of hydrogen bond formation of the amide hydrogens of  $\text{Gdm}^+$  with the carbonyl oxygen of the peptide group is the predominant denaturation mechanism. In other words, the ability of  $\text{Gdm}^+$  to solvate the peptide backbone preferentially leads to protein unfolding. In this sense, both urea and  $\text{Gdm}^+$  must denature proteins by a similar mechanism. We believe that the hydrogen bond between  $\text{Gdm}^+$  and the carbonyl oxygen of the peptide group is stronger than the hydrogen bond between the carbonyl oxygen of urea and the amide protein of the peptide group. As a result,  $\text{Gdm}^+$  is a more efficient denaturing agent than the polar nonelectrolyte urea.

Previous studies have also reached a similar conclusion about the ability of urea to denature proteins,<sup>34,35</sup> namely, that urea preferentially bonds to the backbone rather than disrupting water structure. These studies did not address the importance of the excluded volume of urea in promoting such bonding. As emphasized in our earlier work,<sup>33</sup> excluded volume determines the number of hydrogen bonds that the denaturant makes with the peptide backbone. This in turn determines the efficiency of denaturation.

**Acknowledgment.** D.T. acknowledges partial support of this work by the National Science Foundation through grant number NSF CHE 02-09340.

## References and Notes

- (1) Honig, B.; Sharp, K.; Yang, A. S. *J. Phys. Chem.* **1993**, *97*, 1101.

- (2) Chalikian, T. V.; Volker, J.; Plum, E.; Breuslauer, K. *Proc. Natl. Acad. Sci.* **1999**, *96*, 7853.
- (3) Baldwin, R. L. *Biophys. J.* **1996**, *71*, 2056.
- (4) Arakawa, T.; Timasheff, S. N. *Biochemistry* **1982**, *21*, 6545.
- (5) Collins, K. D. *Proc. Natl. Acad. Sci.* **1995**, *92*, 5553.
- (6) Collins, K. D.; Washabaugh, M. W. *Q. Rev. Biophys.* **1997**, *30*, 241.
- (7) Mason, P. E.; Neilson, G. W.; Dempsey, C. E.; Barnes, A. C.; Cruickshank, J. M. *Proc. Natl. Acad. Sci.* **2003**, *100*, 4557.
- (8) Berendsen, H. J. C.; Grigera, J. R.; Straatsma, T. P. *J. Phys. Chem.* **1987**, *91*, 6269.
- (9) Pettit, B. M.; Rossky, P. J. *J. Chem. Phys.* **1986**, *84*, 5836.
- (10) Hansen, J. P.; McDonald, I. R. *Theory of Simple Liquids*; Academic Press: New York, 1986; p 179.
- (11) Jorgensen, W. L.; Maxwell, D. S.; Triado-Rives, J. *J. Am. Chem. Soc.* **1996**, *118*, 11225; intermolecular potential parameters for the guanidinium ion are found in Supporting Information.
- (12) Straatsma, T. P.; Berendsen, H. C. J. *J. Chem. Phys.* **1988**, *89*, 5876.
- (13) Langer, H.; Offermann, H. *J. Cryst. Growth* **1982**, *60*, 389.
- (14) Boudon, S.; Wipff, G.; Maigret, B. *J. Phys. Chem.* **1990**, *94*, 6056.
- (15) Sangster, M. J. L.; Dixon, M. *Adv. Phys.* **1976**, *25*, 247.
- (16) Schofield, P. *Comput. Phys. Commun.* **1973**, *5*, 17.
- (17) Beeman, D. J. *Comput. Phys.* **1976**, *20*, 130.
- (18) Mountain, R. D.; Brown, A. C. *J. Chem. Phys.* **1985**, *82*, 4236.
- (19) Evans, D. J.; Murad, S. *Mol. Phys.* **1977**, *34*, 327.
- (20) Sonnenschein, R. *J. Comput. Phys.* **1985**, *59*, 347.
- (21) Rapaport, D. C. *J. Comput. Phys.* **1985**, *60*, 306.
- (22) Martyna, G. J.; Klein, M. L.; Tuckerman, M. *J. Chem. Phys.* **1992**, *97*, 2635.
- (23) Leberman, R.; Soper, A. K. *Nature* **1995**, *378*, 364.
- (24) Zhu, S.-B.; Robinson, G. W. *J. Chem. Phys.* **1992**, *97*, 4336.
- (25) Sherman, D. M.; Collings, M. D. *Geochem. Trans.* **2002**, *3*, 102.
- (26) Weerasinghe, S.; Smith, P. E. *J. Chem. Phys.* **2003**, *119*, 11342.
- (27) Driesner, T.; Seware, T. M.; Tironi, I. G. *Geochim. Cosmochim. Acta* **1998**, *62*, 3095.
- (28) Weerasinghe, S.; Smith, P. E. *J. Chem. Phys.* **2004**, *121*, 2180.
- (29) Timasheff, S. N. *Adv. Protein Chem.* **1998**, *51*, 355.
- (30) Kalra, A.; Tugcu, N.; Cramer, S. M.; Garde, S. *J. Phys. Chem. B* **2001**, *195*, 6380.
- (31) Nandi, P. K.; Robinson, D. R. *J. Am. Chem. Soc.* **1972**, *94*, 1299.
- (32) Breslow, R.; Guo, T. *Proc. Natl. Acad. Sci.* **1990**, *87*, 167.
- (33) Mountain, R. D.; Thirumalai, D. *J. Phys. Chem. B* **2004**, *108*, 6826.
- (34) Wallqvist, A.; Covell, D. G.; Thirumalai, D. *J. Am. Chem. Soc.* **1998**, *120*, 427.
- (35) Sharp, K. A.; Madan, B.; Manas, E.; Vanderkooi, J. M. *J. Chem. Phys.* **2001**, *114*, 1791.